



# Defects related to DRAM leakage current studied by electrically detected magnetic resonance

T. Umeda<sup>a,\*</sup>, Y. Mochizuki<sup>a</sup>, K. Okonogi<sup>b</sup>, K. Hamada<sup>b</sup>

<sup>a</sup>*Silicon Systems Research Laboratories, NEC Corporation, 34 Miyukigaoka, Tsukuba 305-8501, Japan*

<sup>b</sup>*Elpida Memory Incorporation, Sagamihara 229-1198, Japan*

## Abstract

The defects responsible for the charge leak of dynamic random access memory (DRAM) memory cells were revealed by a novel type of electrically detected magnetic resonance measurements. The detection sensitivity was greatly improved by using reverse-biased p–n junctions, which enabled us to specify the defect structure. Two types of defects were identified as the origin of the leakage currents; the spin-1 Si dangling-bond (DB) pair in divacancy-oxygen complexes ( $V_2+O$  and  $V_2+O_2$ ) or Si DBs of a different kind from the well-known Si DB center ( $g = 2.0055$ ). It is notable that such defects remain in the device structure in spite of their low thermal stability in Si bulk. © 2001 Elsevier Science B.V. All rights reserved.

**Keywords:** DRAM; Leakage current; Defect; EDMR

## 1. Introduction

In the present and future Si ultralarge scale integrated circuits (ULSIs), process-induced point defects become increasingly crucial, due to downsizing of the device regions as well as complicated processing steps. At present, microscopic information on defects in ULSIs is quite limited. One major reason is that the amount of the defects is far below the detection limit of electron paramagnetic resonance (EPR). Alternatively, electrically detected magnetic resonance (EDMR) technique was developed (for a review see Ref. [1]) and a successful detection of residual defects in Si planar p–n junctions was demonstrated [2]. Since this technique monitors the magnetic resonance of defects via resonant changes in the device current, it is applicable to small sample volumes of ULSIs; moreover, only defects present along the current path and thus related to the device performance can be selectively detected. These advantages make it possible to approach a very few but important defects in actual ULSIs.

We present an EDMR study on the nude  $n^+-p$  junctions of the dynamic random access memory (DRAM) cells. This type of memory device is one of the most sensitive ULSIs to the influence of residual defects. For DRAMs, leakage currents in reverse-biased p–n junctions (junction leakage current, JLC) have to be suppressed in order to keep the capacitor charges as long as possible. The defects in the  $n^+-p$  junctions, however, act as an efficient source of additional JLC. We thus study the defects responsible for the JLC of DRAM cells. In order to directly correlate the defects with the JLC, the key issue is to measure EDMR under a reverse bias, which was very occasionally reported in previous literatures [3]. We carefully examined the reverse-bias characteristic of EDMR and eventually found that the detection under reverse bias is quite possible and even surprisingly sensitive to defects. Based on such EDMR experiments, we discuss the microscopic structures of point defects that cause the JLC.

## 2. EDMR measurements on reverse-biased p–n junctions

Fig. 1 shows the basic structure of the chip examined. This sample mimics the DRAM cells fabricated by the

\*Corresponding author. Tel.: +81-298-50-1548; fax: +81-298-56-6138.

E-mail address: t-umeda@da.jp.nec.com (T. Umeda).

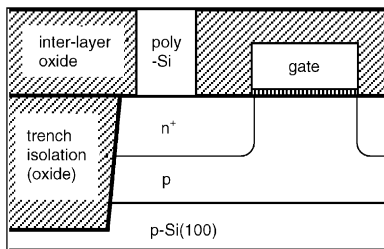


Fig. 1. Sample structure. The p- and n-type regions were produced by the implantation of B and P in a p-type (100) Si wafer.

0.3- $\mu\text{m}$  rule ULSI process. Each cell has an  $n^+p$  junction with an adjacent switching metal-oxide-semiconductor-FET gate. The leakage current of the  $n^+p$  junction is used for EDMR. Our EDMR setup is based on a modified X-band EPR spectrometer [2]. The measurement temperature was carefully determined as follows. At low temperatures, the device current ( $I$ ) decreases due to freeze out of carriers, while a low noise level of the resonant change ( $\Delta I$ ) is achieved due to reduction of the current noise. To gain the highest signal-to-noise ratio and keep the normal current-voltage characteristics, the measurement temperature was set at 230 K. No illumination was done to prevent the generation of photo-excited carriers.

It has been believed that the JLC under reverse bias is unfavorable for EDMR because of the too low current level. However, we found that the reverse JLC becomes extremely sensitive to the defects when high reverse voltages are applied to the junction (Fig. 2). The rate of the resonant current change ( $\Delta I/I$ ) steeply increases over 100 ppm above 5 V. This  $\Delta I/I$  value is much higher than observed under forward biases (30 ppm, independent of the forward bias). The reason why such an enhancement occurred will be simply because the reverse JLC was dominated by the defect-induced leakage currents. In contrast, p-n junctions under forward bias or photo illumination generate only a small fraction of recombination currents related to the defects as compared to the diffusion current. Thus, EDMR under a reverse bias has potential as a powerful technique to raise the defect detection sensitivity.

The location of defects can be known by changing the gate bias. Fig. 3(a) and (a') schematically show a role of the gate bias. When the gate is negatively biased with respect to the p-type substrate, the channel region becomes p-type. Further applying a high negative bias, the p-type layer, and thus depletion layer, expands into the near-surface n-type region (a'). The defects in the newly formed depletion region can cause the JLC and EDMR. Actually, both of the JLC ( $I$ ) and the resonant change ( $\Delta I$ ) are found to increase exponentially with the gate bias [Fig. 3(b)]. This indicates that the defects are

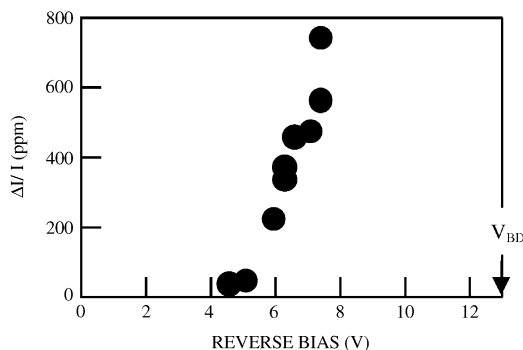


Fig. 2. Reverse bias dependence of the resonant change in a total current ( $\Delta I/I$ ). The magnitude of  $\Delta I/I$  is shown in the peak-to-peak intensity of a first-derivative signal. The gate voltage was set to be  $-3.2\text{ V}$ .  $V_{BD}$  represents the breakdown voltage.

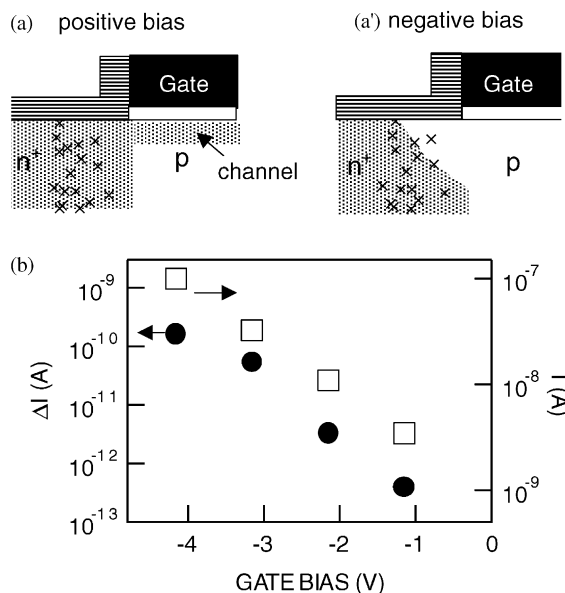


Fig. 3. (a)–(a') Schematic views of the gate-induced expansion of the depletion region. Crosses represent the defects. (b) Gate-bias dependence of  $\Delta I$  (solid circles) and  $I$  (open squares), measured at a reverse bias of 7.3 V.

located in the n-type side of the junction. Also, there is a good correlation between the JLC and  $\Delta I$ .

### 3. Identification of defects

A typical EDMR spectrum for the JLC is shown in Fig. 4(a). The spectrum consists of two parts: one main broad resonance at  $g$  ( $g$  value) = 2.0055 and weak multi lines at the both sides. The main broad signal resembles to those from the well-known Si dangling bond (DB)

observed in amorphous Si [4] and also in Si crystals damaged by implantation [5], radiation [6,7], or mechanical stress [8]. Their isotropic and single-peak features are thought to indicate that the Si DBs are randomly oriented and isolated from each other. However, the same picture of the DBs cannot be applied to the present case, because the  $n^+ - p$  junction of our sample is fully composed of crystalline Si lattice. A similar DB signal has been observed in the other type of planar Si  $p - n$  junctions which are also composed of crystalline Si lattice [2]. In Ref. [2], the DB signal was so weak that detailed spectroscopic features could not be resolved. On the other hand, very-low-noise spectra we obtained [Fig. 4(b)] reveals that the present DB signal really has anisotropy. As seen in the figure, when the external magnetic field (**B**) is aligned to the [100] direction, the peak moves toward lower magnetic field and becomes slightly sharp. This anisotropy evidences that the Si DBs are not randomly oriented in our samples. We consider that the observed anisotropy is related to the crystalline matrix of the relevant Si DBs, which will be studied in detail elsewhere.

The weak multi-lines seen in Fig. 4(a) seem to be a new EDMR signal. We tentatively call it signal A, hereafter. In contrast to the main DB signal, the signal A showed a strong **B** dependence. Fig. 5(a) shows its angular dependence with respect to a magnetic field rotation in the  $(0\bar{1}1)$  plane. One notable character of this pattern is that the ratio between the splitting widths at **B**||[100] and **B**||[110] is just 1:2. This strongly suggests that the signal splitting originates from the fine (electron spin–electron spin) interaction which is nearly

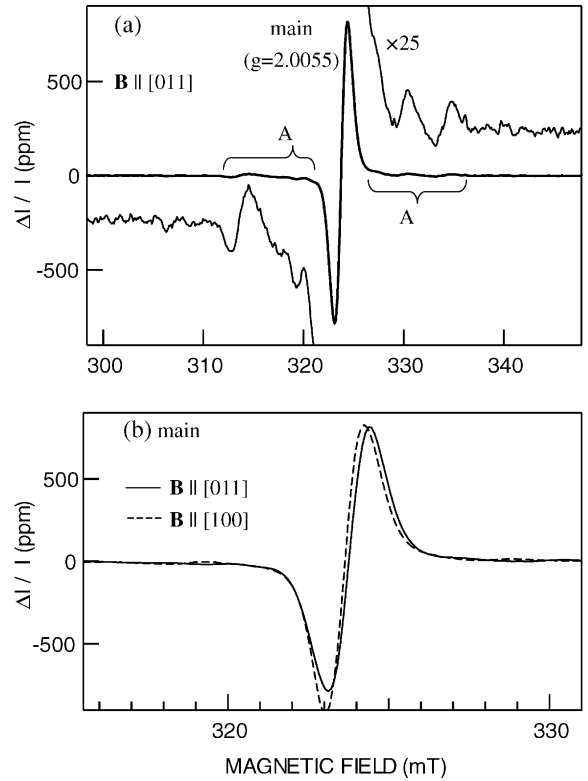


Fig. 4. (a) EDMR spectra for the JLC of the DRAM cells, and (b) the main signal. The magnitude of the JLC was 100 nA at reverse and gate voltages of 7.3 V and  $-4.2$  V, respectively. The spectra in (a) and (b) were measured using the magnetic field modulation of 0.9 and 0.4 mT, respectively.

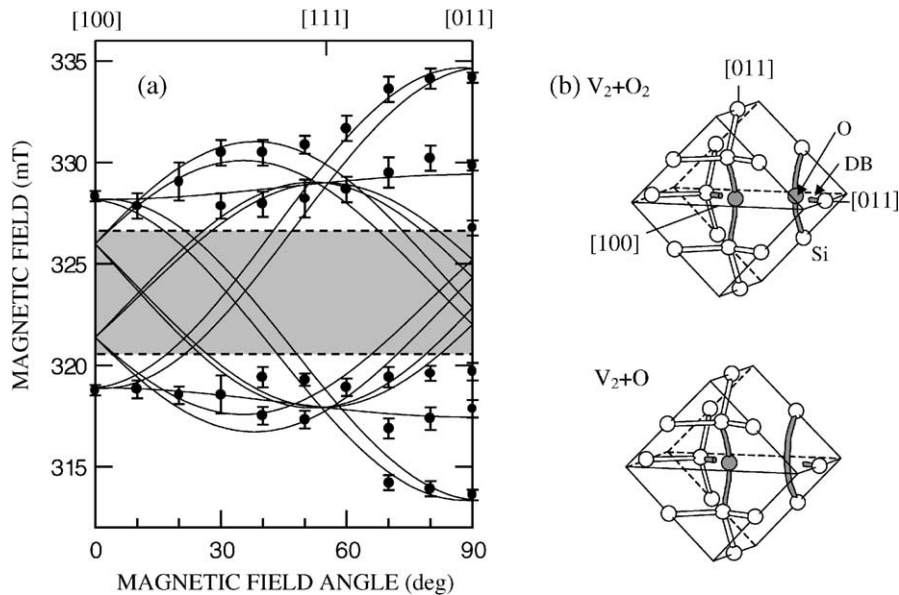


Fig. 5. (a) Angular dependence of the signal A. In the gray area, this signal is not clearly resolved due to the overlapped main signal. (b) The microscopic origins of the signal A.

axial symmetric around the [0 1 1] direction. Previously, similar fine interactions were reported for a series of the spin-1 vacancy-oxygen complexes in radiation damaged Si [9–12]. Such complexes retain a pair of Si DBs, which generate the fine interaction. The solid lines in Fig. 5(a) are calculated by adopting the same defect system known for the divacancy plus one oxygen ( $V_2+O$ , the A14 center) [10] or that plus two oxygen atoms ( $V_2+O_2$ , the P2 center) [9]. The best fit between the calculation and experimental data was obtained with averaged EPR parameters of the two centers. Therefore, we conclude that the signal A originates from a combination of the P2 and A14. The microscopic origins of this signal are given like Fig. 5(b). The oxygen incorporation possibly occurs during the dopant implantation through surface oxides and/or the thermal oxidation process.

Since our chips never received radiation damages or other intentional damages, it is reasonable to consider that the present defects are created by the dopant (phosphorous) implantation. This assignment is also supported by the fact that they are present in the  $n^+$ -type region, which was formed by the ion implantation. After the implantation, our chips were subjected to annealing at a temperature of higher than 800°C. This is much higher than the anneal-out temperature for  $V_2+O$  and  $V_2+O_2$  (<400°C) observed in radiation damaged Si [9]. Also the DB signal ( $g = 2.0055$ ) usually disappears when implantation damaged Si wafers are annealed at the relevant temperature range [5]. Therefore, our observation indicates that the thermal annihilation of the defects is suppressed in the device structures. The device regions are usually surrounded by the substrate surface and isolation structures. These may inhibit the annihilation of the defects.

For the Si DB pairs in  $V_2+O$  and  $V_2+O_2$ , it is reasonable to treat their DBs individually, because of the large separation between the DBs [9]. Also the DB center of  $g = 2.0055$  can be regarded as a single-DB system [2–4]. Thus, we discuss the EDMR mechanism using a simple system, which consists of one carrier and one unpaired electron (an electrically neutral Si DB) in reverse-biased junctions. This system allows only one primary spin-dependent process in which the DB captures a valence-band electron in p-type Si. On the other hand, the carrier generation via the DB (electron emission to the conduction band of n-type Si) is not a spin-dependent process [13]. Therefore, the appearance of the EDMR signals is supposedly a consequence of the electron tunneling from p-type Si to the DB's levels. Such a tunneling probability naturally increases with the reverse voltage. Besides, the relatively high reverse voltage is necessary to extend the depletion region into

the  $n^+$ -region where the DBs are present. We speculate that the drastic signal increase at high reverse voltages is attributed to these factors.

The actual reverse bias for keeping the capacitor charges is typically 1 or 2 V, which is lower than used for EDMR measurements. At such low voltages, the electron tunneling discussed above is largely suppressed. However, the carrier generation via the DB's levels can effectively contribute to the JLC. Therefore, in order to suppress the defect-induced JLC, it is necessary to remove the DBs from the  $n^+$ -region. This will be achieved by optimizing the ion-implantation process and the subsequent annealing.

#### 4. Summary

We have found implantation-induced point defects in the  $n^+$ -p junctions of DRAM cells by means of a novel EDMR technique. The EDMR results clearly showed that such defects are responsible for the JLC in the reverse-biased junctions. The defect structures were assigned to be Si DBs or the spin-1 Si DB pairs of the divacancy-oxygen complexes ( $V_2+O$  and  $V_2+O_2$ ). We pointed out that the thermal annihilation of the defects is suppressed in the device structure than in the bulk, which indicates a significance of probing actual device regions.

#### References

- [1] S. Greulich-Weber, *Mater. Sci. Forum.* 143–147 (1994) 1337.
- [2] T. Wimbauer, K. Ito, Y. Mochizuki, M. Horikawa, T. Kitano, M.S. Brandt, M. Stutzman, *Appl. Phys. Lett.* 76 (2000) 2280.
- [3] F.C. Rong, E.H. Poindexter, M. Harmatz, W.R. Buchwald, G.J. Gerardi, *Solid State Commun.* 76 (1990) 1083.
- [4] T. Umeda, S. Yamasaki, J. Isoya, K. Tanaka, *Phys. Rev. B* 59 (1999) 4849.
- [5] K.L. Brower, W. Beezhold, *J. Appl. Phys.* 43 (1972) 3499.
- [6] M.A. Jupina, P.M. Lenahan, *IEEE Trans. Nucl. Sci.* 36 (1989) 1800.
- [7] D. Vuillaume, D. Deresmes, D. Stievenard, *Appl. Phys. Lett.* 64 (1994) 1690.
- [8] D. Haneman, *Jpn. J. Appl. Phys. (Suppl. 2)* (1974) 371.
- [9] Y.-H. Lee, J.W. Corbett, *Phys. Rev. B* 13 (1976) 2653.
- [10] E.G. Sieverts, J.W. Corbett, *Solid State Commun.* 43 (1982) 41.
- [11] K.L. Brower, *Phys. Rev. B* 4 (1971) 1968.
- [12] W. Jung, G.S. Newell, *Phys. Rev.* 132 (1963) 648.
- [13] F.C. Rong, W.R. Buchwald, E.H. Poindexter, W.L. Warren, D.J. Keeble, *Solid-State Electron.* 34 (1991) 835.